

Cite this: *Energy Environ. Sci.*,  
2026, 19, 1497

# Dynamic reconstruction defines true active states in the hydrogen evolution reaction

Xingyu Ding <sup>ab</sup> and Xianbiao Fu <sup>\*ac</sup>

The hydrogen evolution reaction (HER) plays a pivotal role in sustainable hydrogen production and the transition to a carbon-neutral energy future. Traditionally, HER catalyst design has focused on optimizing as-synthesized structures such as composition, morphology, and electronic states, under the assumption that these features remain static during operation. However, accumulating evidence reveals that HER catalysts undergo profound reconstruction, including phase transformation, compositional change, and atomic rearrangement, which fundamentally redefine the true active states. Neglecting this dynamic evolution risks misidentifying catalytic sites, misinterpreting mechanisms, and misguiding design strategies. In this Perspective, we advocate a reconstruction-centered framework for the HER. We outline key reconstruction modes, argue that reconstruction is thermodynamically driven and shaped by intrinsic and extrinsic factors, and emphasize that catalysts should be designed as precursors engineered to evolve *in situ* into their most active and durable forms. Finally, we advocate for stability assessments that capture steady-state reconstructed phases instead of transient initial states. Adopting this dynamic viewpoint establishes a coherent foundation for mechanistic understanding and rational catalyst design, paving the way toward predictive control of catalytic activity and long-term durability.

Received 30th October 2025,  
Accepted 3rd February 2026

DOI: 10.1039/d5ee06502j

rsc.li/ees

## Broader context

The hydrogen evolution reaction (HER) is a cornerstone of sustainable hydrogen production and the global transition toward a carbon-neutral energy system. Conventional catalyst design has long focused on static structural features such as composition, morphology, and electronic states, assuming that these properties remain unchanged during operation. However, a growing body of evidence reveals that HER catalysts undergo extensive dynamic reconstruction under electrochemical conditions, giving rise to the true active states that govern catalytic performance. Recognizing reconstruction as an intrinsic and thermodynamically driven process prevents the misidentification of active sites, misinterpretation of mechanisms, and misdirection of design strategies, thereby establishing a more coherent and predictive foundation for understanding the hydrogen evolution reaction.

Understanding and controlling reconstruction is therefore essential not only for mechanistic insight but also for ensuring the long-term reliability of catalysts in industrial-scale electrolyzers operating at high current densities. Incorporating reconstruction into catalyst design carries profound implications across multiple scales. At the mechanistic level, it challenges the static view of the HER and calls for frameworks that describe dynamically evolving active states under realistic conditions. At the materials design level, catalysts should be conceived as precursors engineered to evolve into their most active and durable forms, integrating reconstruction principles into synthesis and activation strategies. At the technological level, coupling *operando* diagnostics with controlled synthesis and electrochemical protocols enables the deliberate tuning of reconstruction pathways, promoting activity, stability, and scalability. Looking ahead, emerging concepts such as programmable reconstruction, using time-dependent potentials guided by artificial intelligence (AI)-driven feedback and physics-informed modeling, promise to transform reconstruction from an uncontrolled response into a design variable. Embracing this dynamic perspective provides a unifying framework linking fundamental mechanisms to practical hydrogen technologies, paving the way toward intelligent catalyst systems for the next generation of sustainable energy conversion.

## 1. Introduction

The hydrogen evolution reaction (HER), as the cathodic half of water electrolysis, lies at the heart of renewable hydrogen production.<sup>1</sup> For decades, researchers have pursued better catalysts by tuning the composition, morphology, crystallinity, and electronic states of as-synthesized catalysts.<sup>2–5</sup> These studies implicitly assumed that such static properties persist during operation, and activity–structure relationships have

<sup>a</sup> Department of Materials Science and Engineering, National University of Singapore, Singapore 117576, Singapore. E-mail: xbfu@nus.edu.sg

<sup>b</sup> College of Smart Materials and Future Energy, State Key Laboratory of Coatings for Advanced Equipment, Fudan University, Shanghai 200438, China

<sup>c</sup> Centre for Hydrogen Innovations, National University of Singapore, Singapore 117580, Singapore. E-mail: xbfu@nus.edu.sg



therefore been built on the premise of structural immutability. But are we truly studying the catalysts we design? When the electrochemical environment persistently reshapes catalyst surfaces, can mechanistic models based on static structures remain valid? If catalytic activity and durability ultimately emerge from the reconstructed states, does optimizing pre-catalysts alone still hold meaning? These questions expose the growing inadequacy of the traditional static paradigm.

*Operando/in situ* and post-reaction characterizations consistently reveal extensive structural evolution in HER catalysts, ranging from phase transitions to compositional change, and atomic rearrangement.<sup>6–9</sup> The active state that drives hydrogen production is often fundamentally different from the material first introduced into the electrolyte. This recognition compels a fundamental shift in perspective. Sole reliance on pre-*operando* characterizations risks misidentifying the true active sites; mechanistic models grounded in static snapshots may mislead; and optimizing pre-catalyst structures alone may have limited impact when their evolution is dominated by reconstruction. We therefore call for HER research to explicitly acknowledge reconstruction and to embrace a new paradigm centered on the interplay between dynamic structures and catalytic performance.

In this perspective, we argue that reconstruction is an intrinsic thermodynamically driven phenomenon, not an accidental complication. We classify principal reconstruction modes and analyze their determining factors, then propose a reconstruction-driven framework as a new paradigm for HER catalyst research, linking pre-catalyst structure to reconstruction pathways, and reconstructed active structure to HER performance. This integrated understanding enables rational design of pre-catalysts that evolve into optimal active phases under operating conditions. We also emphasize that only long-term testing captures the steady-state reconstructed structures governing catalytic durability. Through this dynamic perspective, reconstruction transforms from a mechanistic complication into a powerful design principle, unveiling new strategies for advanced HER catalyst development.

## 2. Can we continue to treat reconstruction as peripheral rather than central in HER catalysis?

For decades, mechanistic studies of the HER have rested on a fundamental assumption: synthesized catalysts maintain their structures during the reaction process. This view persisted largely because conventional techniques struggled to resolve the subtle, transient surface changes where the reaction actually proceeds. Within this static paradigm, catalytic activity is directly attributed to pre-catalyst structures.<sup>10</sup> As illustrated in Fig. 1a, HER processes, from reactant adsorption and intermediate formation to hydrogen evolution, are viewed as occurring on structurally invariant catalyst surfaces. Consequently, researchers have developed various descriptors for HER catalyst design, including hydrogen adsorption free energy ( $\Delta G_{\text{H}}$ ), d-band center position,<sup>11–16</sup> work function ( $\Phi$ ), hydrogen binding

energy (HBE),<sup>17,18</sup> and hydroxyl binding energy (OHBE),<sup>19,20</sup> all of which presume structural stability during operation. However, this understanding is increasingly challenged by experimental evidence. *Operando/in situ* and post-reaction characterizations reveal that HER catalysts rarely maintain their pristine states under electrochemical conditions.<sup>6–9</sup> As shown in Fig. 1b, HER is not merely an HER process but involves continuous catalyst surface reconstruction. This means the true active species under operating conditions often differs from the initial catalyst structure.

These reconstruction phenomena can be broadly categorized into three types, each representing different levels of structural evolution. First, phase transformation (Fig. 1c) is defined as a reconstruction process involving changes in crystallographic structure under HER conditions. For example, MoS<sub>2</sub> exemplifies the semiconducting 2H to the metallic 1T conversion under cathodic bias,<sup>21</sup> while transition metal chalcogenides often evolve from chalcogen-rich to chalcogen-poor phases, as in the cubic NiSe<sub>2</sub> to hexagonal NiSe transformation.<sup>22</sup> More broadly, oxides, sulfides, phosphides, carbides, and borides typically reduce to metallic or hydride states that function as the true active phases.<sup>23–35</sup> Earlier studies generally attributed HER activity to metallic species generated under cathodic potentials, exemplified by the transformation of Ni sulfides into Ni metal.<sup>23,24</sup> More recent work has revealed that cathodic bias can also induce the formation of metal hydroxides, with systems such as CoF<sub>2</sub> and CoP converting into Co(OH)<sub>2</sub> as the operative HER phase.<sup>28–32</sup> Second, Compositional change, as illustrated in Fig. 1d, is defined as a reconstruction process involving modification of elemental species and/or ratios while preserving the parent crystal structure. This manifests as a gradual evolution of chemical composition, typically driven by selective dissolution or ion exchange. In multi-metallic systems, electrochemically less stable elements preferentially dissolve, creating thermodynamically more stable surface compositions. A representative example is the Mo element undergoing dynamic dissolution and redeposition on the catalyst surface during HER.<sup>36–39</sup> For example, Du *et al.* reported that NiMo alloys undergo an *in situ* transformation during the HER process, where Mo dissolves as MoO<sub>4</sub><sup>2–</sup>, re-adsorbs and polymerizes into Mo<sub>2</sub>O<sub>7</sub><sup>2–</sup>, and ultimately redeposits to enhance catalytic activity.<sup>36</sup> Similarly, Mo-doped NiP exhibits Mo dissolution and subsequent redeposition, forming new MoO<sub>3</sub> species on the Mo–NiP surface under HER conditions.<sup>39</sup> Third, atomic rearrangement, shown in Fig. 1e, is defined as a reconstruction process involving spatial redistribution of atoms without inducing compositional change. This occurs at highly localized scales, typically resulting from surface or subsurface atom migration under electric fields. Such rearrangement leads to crystalline facet reorganization, which in turn generates surface defects, step edges, elemental segregation, and in extreme cases, surface amorphization. A more extreme case is single-atom catalysts, which are inherently unstable under HER conditions and tend to migrate and aggregate into clusters with lower surface energy. For example, Pt and Ru single atoms have been shown to undergo such atom





Fig. 1 HER models and classification of catalyst reconstruction. (a) Traditional HER model. (b) HER model considering catalyst reconstruction. (c) Phase transformation-type reconstruction. (d) Compositional change-type reconstruction. (e) Atomic rearrangement-type reconstruction.

migration, evolving into cluster states during HER.<sup>40,41</sup> These three reconstruction types are ubiquitous under HER conditions and often occur synergistically. For instance, Ding *et al.* revealed that NiX (X = S or Se) catalysts first undergo a phase transformation into Ni<sub>3</sub>X<sub>2</sub> under cathodic polarization. Subsequently, continuous leaching of surface anions (S or Se) and their replacement by oxygen leads to the formation of NiO, ultimately yielding a Ni<sub>3</sub>X<sub>2</sub>/NiO heterostructure catalyst.<sup>42,43</sup> Notably, the three types of reconstruction discussed above may occur either in the bulk or at the surface. In practice, surface phase transformation and surface compositional change often represent the earliest manifestations of reconstruction under electrochemical conditions, yet they are typically manifested only as amorphous or atomic-scale layers at the surface and therefore remain difficult to detect or unambiguously characterize. By contrast, phase transformation or compositional change occurring in the bulk is generally more readily detectable by conventional structural or spectroscopic techniques, such as X-ray diffraction (XRD) and X-ray absorption spectroscopy (XAS). Even after such bulk reconstruction has taken place, the resulting observations remain inherently bulk-averaged and do not necessarily reflect the true surface state. This underscores the importance of incorporating surface-sensitive characterization techniques, including X-ray photoelectron spectroscopy (XPS), Raman spectroscopy, and time-of-flight secondary ion mass spectrometry (TOF-SIMS), to elucidate dynamic surface reconstruction under electrochemical conditions.

Nevertheless, despite being the equally essential half-reaction to the oxygen evolution reaction (OER) in water splitting, and

although reconstruction has been reported in many HER systems, systematic, predictive, and closed-loop control of reconstruction is still an open challenge and opportunity. We call for increased efforts to systematically unveil HER catalyst reconstruction: in the short term, identifying and cataloging reconstruction types and manifestations across different systems; in the long term, distilling universally applicable reconstruction mechanisms from extensive studies, establishing reliable dynamic structure–performance relationships, and ultimately developing new paradigms for HER catalyst design that harness reconstruction processes.

### 3. HER catalyst reconstruction: accident of operation or inevitable thermodynamic pathway?

The ubiquity of reconstruction in HER catalysts raises a fundamental question: Is reconstruction merely an operational perturbation or a thermodynamically inevitable evolution? From an energetic perspective, catalyst surface reconstruction represents not random events but the system's spontaneous pursuit of lower free energy states under specific conditions. As illustrated in Fig. 2a, we propose a lifecycle model encompassing catalyst reconstruction from synthesis through HER operation to post-reaction states. Freshly as-prepared catalysts exposed to ambient atmosphere inevitably undergo mild reconstruction through oxidation or species adsorption from air, reducing surface energy. Upon immersion in electrolyte at open circuit potential (OCP), catalyst surfaces interact with the solution



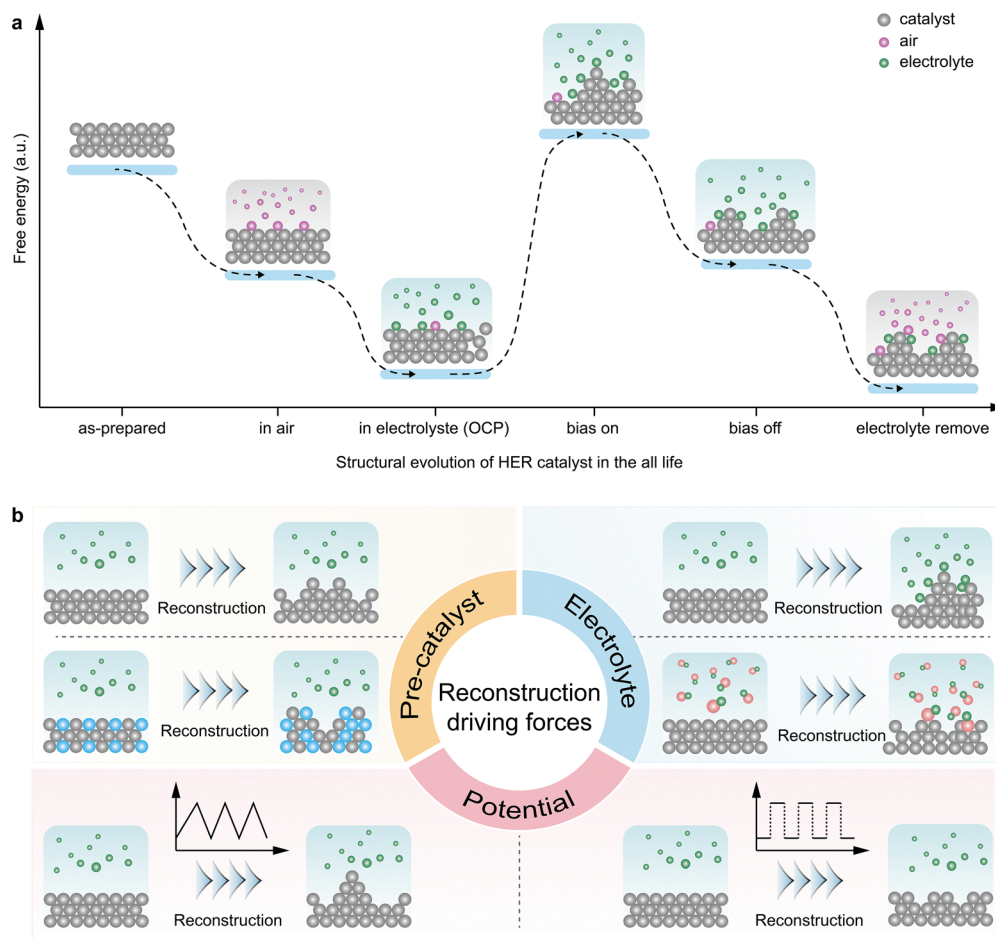


Fig. 2 Thermodynamic origins and driving forces of catalyst reconstruction in HER. (a) Schematic illustration of the free-energy evolution throughout the catalyst lifecycle, from synthesis to operation. (b) Catalyst reconstruction driven by pre-catalyst structure, electrolyte environment, and applied potential.

environment through species adsorption or chemical corrosion, primarily from  $H^+$  or  $OH^-$  interactions in HER, driving further reconstruction and surface energy minimization. For example, Ledendecker *et al.* show that non-noble materials such as  $MoS_2$ ,  $Ni_5P_4$ , WC, and  $Co_2P$  undergo significant metal dissolution at open circuit, demonstrating their intrinsic instability under OCP.<sup>44</sup> When cathodic bias initiates HER, the system's electrochemical potential shifts dramatically. Surface atoms become activated and reorganize through intense electrolyte interactions, forming higher energy excited states that subsequently relax into metastable structures sustainable under reaction conditions. Critically, the true catalytically active sites exist within these metastable configurations. Upon bias removal, the system's free energy changes again, destabilizing these metastable states and driving structural relaxation toward lower surface energy configurations compatible with the new environment. Finally, when catalysts are removed from the electrolyte, rinsed, and dried, these structures undergo further reconstruction through air exposure, continuing their evolution toward thermodynamic minima.

This lifecycle model reveals that reconstruction pervades every stage from catalyst synthesis through HER operation,

naturally raising critical questions: What factors govern surface reconstruction behavior and thus active site formation? Can we identify universal principles to deliberately control reconstruction for optimal electrocatalytic performance? Understanding this model proves essential for mastering surface reconstruction and advancing HER catalysis. Three interconnected factors emerge as reconstruction drivers: pre-catalyst structure, electrolyte environment, and applied potential. Pre-catalyst structure manifests through intrinsic atomic properties that dictate responses to electrochemical stimuli (Fig. 2b). Even identical elements exhibit divergent reconstruction behaviors depending on initial atomic arrangements; crystalline facets, defect densities, and coordination environments all influence transformation pathways. For example, while cubic  $CoSe_2$  remains stable under HER operating conditions, P-doped  $CoSe_2$  can be induced to generate metallic  $Co^0$  as the catalytically active species.<sup>45</sup> Electrolyte environment creates distinct reconstruction trajectories even for identical precursors under the same potential (Fig. 2b). This arises from surface-specific adsorption during HER, which modulates atomic properties and triggers divergent restructuring. Leveraging this principle, surface reconstruction can be indirectly controlled by tuning the pH,



introducing additives with tailored adsorption affinities, or employing electrochemically inert species.<sup>46–49</sup> For example, Sun *et al.* examined the pH-dependent reconstruction of  $\text{Co}_{0.5}\text{W}_{0.5}\text{S}_x$ . Under neutral or alkaline conditions, the bulk converted to  $\text{CoO}$  and the surface to  $\text{CoO}/\text{Co}(\text{OH})_2$ , whereas in acid, only the surface was reconstructed.<sup>46</sup> Other studies report that adding extra  $\text{MoO}_4^{2-}$  to Mo-based HER catalysts, such as  $\text{MoSe}_2$  or  $\text{Mo}_2\text{Co}_3\text{O}_8$ , facilitates surface reconstruction into active  $\text{Mo}_2\text{O}_7^{2-}$  species.<sup>47,48</sup> Beyond deliberate manipulation of bulk electrolyte composition, the electrolyte environment itself exhibits pronounced dynamic evolution during the HER, particularly within the localized interfacial region, which may in turn influence catalyst restructuring pathways.<sup>50,51</sup> The sustained consumption of protons during HER inevitably establishes local pH gradients.<sup>52,53</sup> Such dynamically evolving interfacial pH directly modulates surface protonation states, adsorption energetics, and phase stability, thereby providing thermodynamic driving forces for catalyst restructuring. Consistent with this perspective, Bao *et al.* demonstrated that the locally acidic interfacial environment generated under HER conditions can induce the transformation of  $\text{WO}_2$  into  $\text{H}_x\text{WO}_y$ , establishing a direct link between pH dynamics and specific restructuring pathways.<sup>54</sup> The electrolyte conductivity during HER is likewise not static. HER-induced concentration polarization, particularly the nucleation, growth, and accumulation of hydrogen bubbles, intermittently disrupts ionic conduction pathways, elevates effective ohmic resistance, and redistributes local current density and overpotential, thereby inducing divergent catalyst restructuring trajectories.<sup>1,55</sup> Concurrently, sustained  $\text{H}_2$  evolution exerts physical impingement that drives morphological restructuring or even mechanical disintegration and detachment of catalysts.<sup>56</sup> Moreover, the sequential processes of  $\text{H}_2$  generation, dissolution, supersaturation, bubble formation, and detachment give rise to variations in the interfacial microenvironment, including local pH fluctuations, mass transport limitations, and active site blockage. This cascade of microenvironmental evolution collectively influences catalyst restructuring pathways.<sup>55</sup> Although studies directly correlating electrolyte dynamics with catalyst restructuring pathways remain limited, particularly regarding the effects of local conductivity variations and bubble evolution on dynamic catalyst restructuring, these analyses collectively underscore that electrolyte evolution and catalyst restructuring constitute intrinsically coupled and inseparable processes during prolonged HER operation. Applied potential serves as the primary energetic driver, directly programming reconstruction pathways (Fig. 2b). It controls energy input across reaction stages, determining initial excited states and sustainable metastable configurations, ultimately dictating the reconstruction direction. Notably, Gisbert-González *et al.* revealed that applied bias regulates surface hydrogen coverage, leading to systematic evolution of the catalytic transition state. This finding suggests that electrochemical potential provides a powerful lever to control transition states and, in turn, direct catalyst reconstruction pathways.<sup>57</sup> For example, under HER conditions at overpotentials below 500 mV,  $\text{NiS}_2$  transforms into the active

$\text{Ni}_3\text{S}_2$  phase. Feng *et al.* demonstrated that higher overpotentials produce a  $\text{Ni}/\text{Ni}_3\text{S}_2$  composite, dramatically boosting HER activity.<sup>58</sup>

Current efforts have revealed diverse reconstruction behaviors, yet predictive and programmable control over reconstruction remains insufficiently developed. We advocate for more systematic investigations on how initial structures influence reconstruction pathways, how electrolyte environment directs transformation, and how potential protocols control evolution.

#### 4. If reconstruction redefines the active state, can we trust short-term stability tests?

In the preceding sections, we discussed whether HER catalysts reconstruct and the driving forces behind this process, yet the extent of reconstruction has received little attention. As illustrated in Fig. 3a, a central unresolved question is whether reconstruction under HER conditions is confined to the surface, penetrates into the subsurface, or ultimately transforms the entire structure. The depth of reconstruction dictates the spatial distribution and stability of active sites, making it a critical determinant of both mechanism and design. However, systematic studies of reconstruction extent in HER catalysts remain scarce, leaving an important gap.

This gap is compounded by the dominance of short-term stability tests, typically lasting only a few to several tens of hours (Fig. 3b). While convenient, such protocols overlook the ongoing structural evolution of catalysts. Early activity often reflects transient states rather than the steady reconstructed configurations that define durability. In fact, the most active or stable phases may only emerge after extended reconstruction, far beyond conventional testing windows. Catalysts that initially appear robust may later deactivate, while others with modest initial activity may evolve into highly durable systems (Fig. 3b).

As shown in Fig. 3b, we argue that HER stability assessment requires a paradigm shift. Long-term testing is indispensable to capture the kinetics of reconstruction and the durability of the reconstructed states. By combining extended *operando* characterization with electrochemical measurements, researchers can identify when reconstruction reaches completion and evaluate whether the resulting phases sustain activity or drift toward deactivation. Before assessing reconstruction depth, it is essential to establish whether the catalyst has reached a stable reconstructed state. *Operando* or *in situ* spectroscopic techniques, such as Raman spectroscopy, XAS, and XRD, enable real-time tracking of structural and chemical-state evolution during operation. The convergence of these spectroscopic signatures under prolonged operating conditions provides a key criterion for identifying reconstruction completion. Complementarily, *operando* TOF-SIMS can monitor the dynamic evolution of surface and near-surface species, offering additional insight into whether reconstruction has reached a steady state. In parallel, the stabilization of electrochemical parameters, including current





Fig. 3 Reconstruction extent and stability evaluation of HER catalysts. (a) Possible outcomes of catalyst reconstruction with varying extents. (b) Correlation between HER activity, reconstruction state, and testing time during stability evaluation.

density evaluated by linear sweep voltammetry (LSV), cyclic voltammetry (CV), or chronopotentiometry (CP), the Tafel slope derived from polarization analysis, and impedance features probed by electrochemical impedance spectroscopy (EIS), serves as an electrochemical indicator of reconstruction completion.<sup>5</sup> Once a steady reconstructed state is established, *ex situ* characterization can be employed to resolve the spatial depth of reconstruction. Surface-sensitive techniques, such as angle-resolved XPS and depth-profiling methods (*e.g.*, Ar<sup>+</sup> sputtering XPS and TOF-SIMS), reveal compositional gradients from the surface to subsurface regions, while cross-sectional transmission electron microscopy (TEM) combined with electron energy loss spectroscopy (EELS) mapping enables direct visualization of reconstructed domains. For crystalline phase evolution, grazing-incidence XRD probes near-surface structural changes, whereas conventional XRD reflects bulk phase behavior, allowing surface and bulk reconstruction to be distinguished.

Such an approach establishes a more rigorous definition of stability, grounded in the intrinsic properties of reconstructed catalysts rather than in transient behavior. Recognizing durability as inseparable from reconstruction, we call for long-term stability testing to be established as a new standard for HER catalysis, enabling the rational development of catalysts capable of delivering sustained performance under realistic operating conditions.

## 5. From static illusions to dynamic realities: establishing a reconstruction-driven paradigm for HER catalysts

The pervasive and thermodynamically driven nature of reconstruction fundamentally challenges traditional HER research

frameworks: so-called “static” catalysts are merely transition states, while true catalytic identity is progressively established through reconstruction under electrochemical conditions. Ignoring this dynamic evolution leads to misidentification of active sites, as true catalytic phases often emerge only during operation; mechanistic model deviations, since kinetic features (Tafel slopes, reaction orders) likely reflect reconstructed rather than pristine states; and design inefficiencies, because optimizing pre-catalysts alone yields limited benefits when reconstruction dominates final identity. The key imperative going forward is to harness structural evolution as a tool for performance enhancement rather than treating it as an uncontrolled variable. As shown in Fig. 4, we propose a research paradigm that systematically correlates pre-catalyst structures, *operando*-evolved active structures, and HER performance. This approach comprises three integrated steps: (i) elucidating structure–reconstruction relationships by mapping how the pre-catalyst transforms under electrochemical conditions into their active forms, and (ii) establishing structure–performance correlations between reconstructed active phases and HER performance. Building on these two research steps, (iii) pre-catalyst can be rationally designed *via* composition and structure regulation (*e.g.*, doping, facet engineering, defect engineering, and hetero-junction construction), in combination with operational parameters such as electrolyte composition (pH, ionic species) and applied potential to steer reconstruction toward optimal catalytic configurations. This pre-catalyst structure–active structure–HER performance framework, detailed in the following section, provides a comprehensive blueprint for advancing HER catalyst development.

We begin with step (i), where the key objective is to resolve the pre-catalyst structure and the active structure formed under defined operational parameters such as electrolyte composition



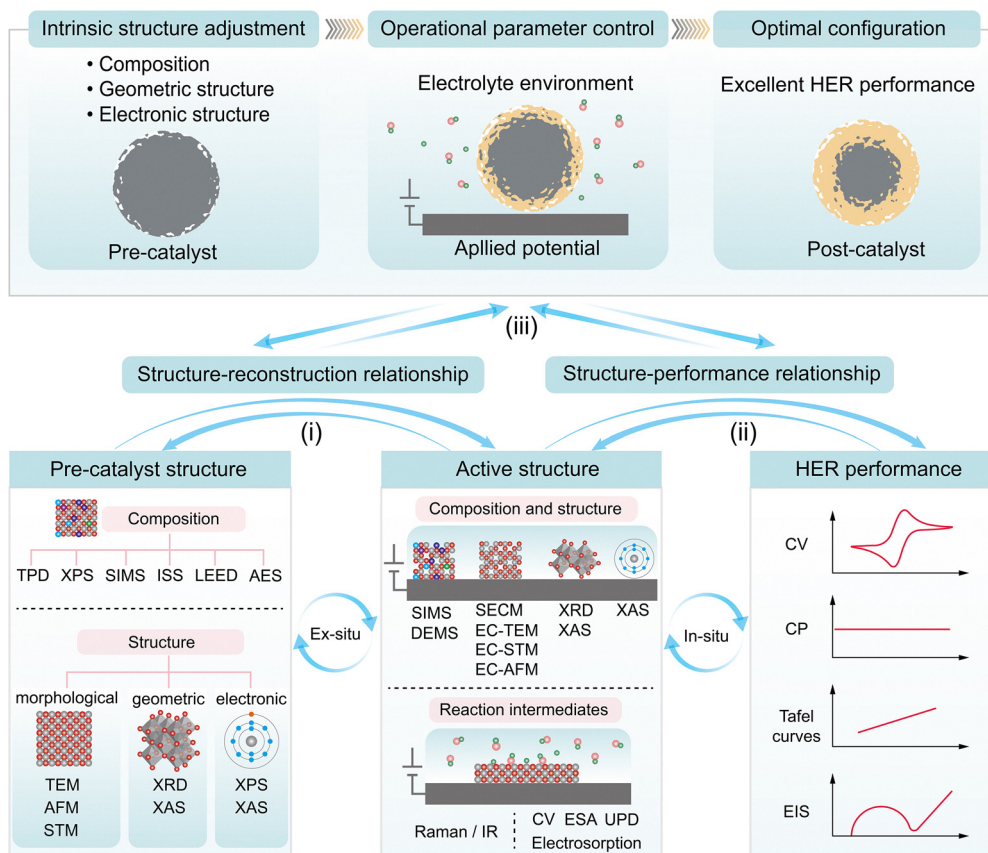


Fig. 4 Design paradigm of HER catalysts based on reconstruction. Step (i): structure–reconstruction relationship. Step (ii): structure–performance relationship. Step (iii): directed reconstruction via intrinsic pre-catalyst structure factors and extrinsic operational parameters regulation toward excellent HER performance.

(pH, ionic species) and applied potential, in order to establish their structural relationship. Elucidating these structures necessitates an integrated characterization strategy that combines bulk and surface probes, with priority given to surface-sensitive techniques, since catalytic function is ultimately defined at the surface. A rigorous understanding of the pre-catalyst requires comprehensive *ex situ* characterization. Surface-sensitive probes such as temperature-programmed desorption (TPD), XPS, SIMS, ion scattering spectroscopy (ISS), low-energy electron diffraction (LEED), and Auger electron spectroscopy (AES) resolve surface composition, while TEM, atomic force microscopy (AFM), and scanning tunneling microscopy (STM) uncover morphological structure. Complementarily, bulk-sensitive techniques, including XRD and XAS, reveal long-range crystallinity and local coordination geometric structure, with XPS and XAS jointly elucidating electronic structure. For the active structure, *operando* or *in situ* techniques are essential for tracking its dynamic evolution under HER conditions. *In situ* TOF-SIMS and differential electrochemical mass spectrometry (DEMS) capture compositional changes; scanning electrochemical microscopy (SECM), electrochemical transmission electron microscopy (EC-TEM), electrochemical scanning tunneling microscopy (EC-STM), and electrochemical atomic force microscopy (EC-AFM) monitor surface restructuring of morphological structure in real time;

*in situ* XRD probes global phase transitions; and *in situ* XAS simultaneously provides information on local geometric and electronic structure under HER conditions. Integrating these experimental insights with theoretical modeling enables the mapping of explicit structure–reconstruction relationships, bridging pre-catalyst attributes, operational environments, and reconstructed configurations. The step (ii) of this paradigm focuses on the structure–performance correlation of reconstructed active phases. While delineating the transformation pathways of pre-catalysts is essential, the ultimate objective is to quantitatively link these reconstructed states to HER performance metrics, including overpotential, Tafel slope, exchange current density, and long-term stability. Establishing such structure–activity relationships requires, beyond identifying the *operando* active structure in step (i), direct probing of reaction intermediates, including  $\text{H}_2\text{O}^*$ ,  $\text{H}^*$ , and  $\text{OH}^*$  adsorption. *Operando* techniques that can capture these intermediates, such as Raman spectroscopy and infrared spectroscopy (IR), are therefore indispensable. In addition, electrochemical probe techniques such as CV, electrochemical stripping analysis (ESA), underpotential deposition (UPD), electrosorption, and EIS can provide complementary insights into surface states and adsorbed intermediates under HER conditions, by revealing changes in active site availability, adsorption behavior, and



surface reconstruction.<sup>59–64</sup> When combined with theoretical calculations, these approaches reveal the HER pathways on reconstructed active surfaces and enable the rational derivation of structure–performance correlations and mechanistic insights. Together, steps (i) and (ii) establish a unified “pre-catalyst structure–reconstructed active structure–HER performance” framework, turning reconstruction from an uncontrolled variable into a design tool. Building on this foundation, step (iii) elevates the paradigm to a prescriptive strategy: a reverse-engineering strategy identifies optimal reconstructed states, then directs the design of pre-catalyst structures (composition, geometric and electronic structure, *etc.*), electrolytes (pH, ionic species, *etc.*), and applied potentials to achieve it. By treating *operando* reconstruction as a feature rather than a limitation, this paradigm offers a pathway to simultaneously maximize activity and durability.

## 6. Conclusion and outlook

In summary, this perspective calls for increased attention to the dynamic reconstruction of HER catalysts. Future studies should broaden the range of material systems, expand the catalog of reconstruction types, and deepen understanding of how pre-catalyst structure, electrolyte environment, and applied potential govern reconstruction, enabling deliberate and directional control. Stability evaluations should be extended to ensure catalysts reach their fully reconstructed state, reflecting true durability. Ultimately, the research paradigm for HER catalysis must shift from static catalysts toward dynamic, reconstruction-driven catalysts, fostering a more accurate understanding of intrinsic activity and long-term stability.

While the reconstruction-driven paradigm offers a prescriptive framework for HER catalyst design, its experimental validation is often constrained by limited access to specialized *operando* spectroscopies. Techniques such as *in situ* Raman, XPS, XAS, and IR typically require substantial capital investment, complex infrastructure, and sustained access to vacuum or synchrotron facilities, which are resources not universally available. This perspective therefore emphasizes complementary, broadly accessible *operando* electrochemical probes, including CV, ESA, UPD, electrosorption, and EIS, that can resolve surface site evolution, adsorption dynamics, and interfacial kinetic signatures without reliance on large-scale facilities. These techniques require only standard instrumentation available in most electrochemistry laboratories, namely a three-electrode cell and a commercial potentiostat. *Operando* CV tracks potential-resolved redox peak evolution to fingerprint phase conversion or coordination changes during reconstruction. ESA quantifies reconstruction-induced variations in active site availability by integrating stripping charges from oxidative removal of adsorbed species. UPD, implemented in dilute electrolytes (<5 mM trace metal ions) with slow-scan voltammetry, resolves facet- and site-selective adsorption energetics, constraining phase persistence and interfacial stability. Electrosorption under inert electrolytes and discrete potential

holds probes potential-dependent adsorption of non-complexing spectator ions, capturing interfacial state transitions accompanying reconstruction. Among various electrochemical characterization techniques, EIS, as a non-invasive, frequency-resolved, and readily implementable *operando* technique, has been extensively employed to investigate the dynamic reconstruction of OER catalysts.<sup>65–67</sup> This methodology can be equally applicable to HER catalysts. By analyzing the frequency-dependent impedance response, EIS enables discrete extraction of charge transfer kinetics ( $R_{ct}$ ) in the high-frequency region, interfacial capacitance characteristics ( $C_{dl}$ ) in the mid-frequency region, and mass transport limitations coupled with bubble coverage effects in the low-frequency region ( $Z_w$ ).<sup>68</sup> The temporal or potential-dependent evolution of these parameters serves as indirect yet highly sensitive fingerprint signatures of catalyst surface reconstruction. Mechanistically, a progressive decrease in  $R_{ct}$  typically signifies the formation of more active phases, while significant  $C_{dl}$  variations reflect the evolution of electrochemically active surface area (ECSA), intimately associated with surface roughening, layer exfoliation, or exposure of new active sites.<sup>69</sup> In the low-frequency regime, the  $Z_w$  response exhibits particular sensitivity to bubble dynamics and local mass transfer heterogeneity, enabling discrimination between intrinsically kinetic-limited and diffusion or hydrodynamically dominated regimes.<sup>70</sup> Recent HER studies have unambiguously demonstrated the intrinsic correlation between these EIS features and catalytic kinetics.<sup>69–74</sup> For instance, *operando* EIS tracking of H-TaS<sub>2</sub> revealed progressive reduction in  $R_{ct}$  and increased effective  $C_{dl}$ , evidencing self-optimizing morphological reconstruction through layer thinning and basal plane activation that promotes HER kinetics.<sup>69</sup>

In addition, while fundamental understanding of HER catalyst reconstruction has advanced considerably, translating these insights into industrial electrolyzers operating at high current densities (> 500 mA cm<sup>-2</sup>) remains challenging.<sup>75–77</sup> In practical electrolyzers, catalysts experience hydrodynamic and electrochemical environments fundamentally different from laboratory three-electrode cells. Local flow fields governed by electrolyzer architecture, including serpentine and parallel channels as well as flow by and flow through configurations and channel geometry, directly influence mass transport, local pH gradients, and interfacial electric fields.<sup>78</sup> High-current-density operation brings elevated local temperatures, intensified electric fields, and enhanced mass transport, while vigorous bubble nucleation, growth, and detachment impose periodic mechanical stresses and generate transient concentration gradients.<sup>79–81</sup> As discussed, applied potential, electrolyte environment, and pre-catalyst structure govern reconstruction pathways; flow field design and bubble dynamics indirectly yet profoundly influence these driving forces by modulating local potential distribution and electrolyte environment (*e.g.*, interfacial pH and ionic concentration). However, direct investigations of the effects of flow field design, bubble dynamics, and electrolyzer architecture on catalyst reconstruction remain scarce. Existing reconstruction studies are largely performed in simplified three-electrode systems, while studies on flow fields and bubble behavior mainly address mass transport and reaction kinetics. Bridging



this gap by correlating electrolyzer environment, reconstruction behavior, and catalytic performance will open new opportunities for reconstruction-guided industrial catalyst design. First, engineering flow fields and channel geometry to homogenize local environments (potential, pH, ionic concentration) can minimize reconstruction heterogeneity across electrodes. Second, the design of reconstruction ready catalyst precursors that take advantage of high current density conditions, such as elevated temperatures, intensified fields, and enhanced mass transport, enables their rapid evolution into reconstructed phases that combine high activity with mechanical robustness.<sup>82–84</sup> Third, coupling reconstruction understanding with accelerated stress tests mimicking industrial transients (load cycling, start-up/shut-down) enables more predictive durability assessments.<sup>85,86</sup> Incorporating hydrodynamic, thermal, and mechanical factors into the reconstruction framework, future research can bridge fundamental understanding and rational design, enabling HER catalysts for sustained high-rate hydrogen production in real-world electrolyzers.

Looking ahead, the next Frontier in HER catalysis lies in actively controlling rather than passively observing catalyst reconstruction. We envision a new paradigm, termed Programmable Reconstruction, that treats catalyst evolution as an actively tunable process instead of an inevitable structural response. Wu *et al.* showed that square-wave potentials rapidly reconstruct oxide precursors into active metal/oxide heterointerfaces with superior efficiency and scalability over constant potential, validating a blueprint for Programmable Reconstruction.<sup>87</sup> The emerging concept of programmable electrochemical potentials offers a route to realize Programmable Reconstruction by modulating atomic migration and interfacial phase transformation pathways, encoding reconstruction kinetics as a controllable design parameter.<sup>88</sup> This is achieved through potential waveform engineering in the time and frequency domains, in line with the pulsed electrolysis framework articulated by Casebolt and colleagues. Detailly, time-domain potential pulses defined by amplitude, frequency, and duty cycle periodically amplify interfacial electric fields, accelerating atomic mobility and inducing defects at programmed densities. Frequency-domain excitation using characteristic frequencies and harmonics can be synchronized with intrinsic time scales of surface atom rearrangement or metastable phase formation, selectively activating reconstruction branches. When coupled with artificial intelligence (AI)-driven *operando* diagnostics, such as adaptive spectroscopic feedback and automated potential modulation, real-time mapping and control of dynamic structure–function relationships will become feasible.<sup>88</sup> Sheng *et al.* demonstrate essential components of a closed-loop system by establishing an autonomous electrochemical platform where real-time signal streams inform AI-enabled state inference and actuate adaptive potential control, indicating the practical potential of closed-loop regulation for catalyst reconstruction.<sup>89</sup> Furthermore, physics-informed inverse modeling powered by machine learning (ML) can reconstruct free-energy landscapes from *operando* data, revealing hidden metastable intermediates and predicting optimal excitation patterns for targeted reconstruction. To operationalize

this goal, Bayesian optimization-guided, ML-driven waveform search provides a concrete, executable approach to efficiently explore pulsed-potential spaces and iteratively refine adaptive waveforms that align with inverse-inferred energetic and kinetic targets, enabling practical AI-assisted training of HER catalyst reconstruction pathways.<sup>90</sup> Based on this analysis, we propose an editable closed-loop workflow for HER catalyst reconstruction. (1) Acquire *operando* signals to track evolving interfaces. (2) Use AI state inference to identify stages and update descriptors. (3) Apply ML-based inverse modelling to map free energies and predict target phases and excitation motifs. (4) Perform automated waveform actuation in time/frequency domains. (5) Refine waveforms *via* adaptive AI feedback to steer catalysts toward desired reconstructed active phases under operating conditions.<sup>88</sup> By integrating these tools, reconstruction can evolve from an intrinsic response into a programmable feature, a data-driven, feedback-controlled paradigm for catalyst evolution. Ultimately, embracing programmable reconstruction will enable the rational “training” of catalysts to self-organize into thermodynamically favorable yet kinetically optimized active states, paving the way toward intelligent catalyst systems for scalable and durable hydrogen technologies.

## Author contributions

X. Fu conceptualized the work, supervised the project, and revised the manuscript. X. Ding wrote the original draft and prepared the figures. All authors discussed the content and approved the final version

## Conflicts of interest

The authors declare no competing interests.

## Data availability

The authors declare that the data supporting the finding of this study are available in this paper.

## Acknowledgements

The authors acknowledge support from the startup grant provided by the National University of Singapore. X. Ding is grateful for funding sponsored by Shanghai Sailing Program under Grant No. 24YF2701900.

## Notes and references

- 1 M. Chatenet, B. G. Pollet, D. R. Dekel, F. Dionigi, J. Deseure, P. Millet, R. D. Braatz, M. Z. Bazant, M. Eikerling, I. Staffell, P. Balcombe, Y. Shao-Horn and H. Schäfer, *Chem. Soc. Rev.*, 2022, **51**, 4583–4762.
- 2 Y. Liu, Y. Guo, Y. Liu, Z. Wei, K. Wang and Z. Shi, *Energy Fuels*, 2023, **37**, 2608–2630.



- 3 Y. Luo, Y. Zhang, J. Zhu, X. Tian, G. Liu, Z. Feng, L. Pan, X. Liu, N. Han and R. Tan, *Small Methods*, 2024, **8**, 2400158.
- 4 J. Zhang, C. Ma, S. Jia, Y. Gu, D. Sun, Y. Tang and H. Sun, *Adv. Energy Mater.*, 2023, **13**, 2302436.
- 5 M. A. Qadeer, X. Zhang, M. A. Farid, M. Tanveer, Y. Yan, S. Du, Z.-F. Huang, M. Tahir and J.-J. Zou, *J. Power Sources*, 2024, **613**, 234856.
- 6 Y. Zeng, M. Zhao, Z. Huang, W. Zhu, J. Zheng, Q. Jiang, Z. Wang and H. Liang, *Adv. Energy Mater.*, 2022, **12**, 2201713.
- 7 W. Zhang, Y. Yang, Y. Tang and Q. Gao, *J. Energy Chem.*, 2022, **70**, 414–436.
- 8 R. Zhang, B. Qian, K. Xu, A. Said, K. Chen, C. Yang, S. Komarneni and D. Xue, *Rev. Mater. Res.*, 2025, **1**, 100045.
- 9 Z. Li, X. Ding, D. Liu, J. Zhou, Y. Gao, Y. Liu, L. Jiang, R. Wu and H. Pan, *Mater. Sci. Eng., R*, 2025, **166**, 101061.
- 10 Y. Zheng, Y. Jiao, A. Vasileff and S.-Z. Qiao, *Angew. Chem., Int. Ed.*, 2018, **57**, 7568–7579.
- 11 N. Du, C. Wang, X. Wang, Y. Lin, J. Jiang and Y. Xiong, *Adv. Mater.*, 2016, **28**, 2077–2084.
- 12 C. Wei, Y. Sun, G. G. Scherer, A. C. Fisher, M. Sherburne, J. W. Ager and Z. J. Xu, *J. Am. Chem. Soc.*, 2020, **142**, 7765–7775.
- 13 Z. Chen, Y. Song, J. Cai, X. Zheng, D. Han, Y. Wu, Y. Zang, S. Niu, Y. Liu, J. Zhu, X. Liu and G. Wang, *Angew. Chem., Int. Ed.*, 2018, **57**, 5076–5080.
- 14 C. Miao, Y. Zang, H. Wang, X. Zhuang, N. Han, Y. Yin, Y. Ma, M. Chen, Y. Dai, S. Yip, J. C. Ho and Z.-X. Yang, *Adv. Mater. Interfaces*, 2022, **9**, 2200739.
- 15 Y. Wang, X. Li, M. Zhang, Y. Zhou, D. Rao, C. Zhong, J. Zhang, X. Han, W. Hu, Y. Zhang, K. Zaghbi, Y. Wang and Y. Deng, *Adv. Mater.*, 2020, **32**, 2000231.
- 16 I. S. Kwon, I. H. Kwak, G. M. Zewdie, S. J. Lee, J. Y. Kim, S. J. Yoo, J.-G. Kim, J. Park and H. S. Kang, *Adv. Mater.*, 2022, **34**, 2205524.
- 17 W. Sheng, M. Myint, J. G. Chen and Y. Yan, *Energy Environ. Sci.*, 2013, **6**, 1509–1512.
- 18 W. Sheng, Z. Zhuang, M. Gao, J. Zheng, J. G. Chen and Y. Yan, *Nat. Commun.*, 2015, **6**, 5848.
- 19 I. T. McCrum and M. T. M. Koper, *Nat. Energy*, 2020, **5**, 891–899.
- 20 J. Zhang, L. Zhang, J. Liu, C. Zhong, Y. Tu, P. Li, L. Du, S. Chen and Z. Cui, *Nat. Commun.*, 2022, **13**, 5497.
- 21 Y. Zhao, H. Li, R. Yang, S. Xie, T. Liu, P. Li, Y. Liu, H. Li, F. Yang and T. Zhai, *Energy Environ. Sci.*, 2023, **16**, 3951–3959.
- 22 L. Zhai, T. W. Benedict Lo, Z.-L. Xu, J. Potter, J. Mo, X. Guo, C. C. Tang, S. C. Edman Tsang and S. P. Lau, *ACS Energy Lett.*, 2020, **5**, 2483–2491.
- 23 Q. Ma, C. Hu, K. Liu, S.-F. Hung, D. Ou, H. M. Chen, G. Fu and N. Zheng, *Nano Energy*, 2017, **41**, 148–153.
- 24 C. Hu, Q. Ma, S.-F. Hung, Z.-N. Chen, D. Ou, B. Ren, H. M. Chen, G. Fu and N. Zheng, *Chem*, 2017, **3**, 122–133.
- 25 R. Wu, H. Liu, J. Xu, M.-R. Qu, Y.-Y. Qin, X.-S. Zheng, J.-F. Zhu, H. Li, X.-Z. Su and S.-H. Yu, *Adv. Energy Mater.*, 2025, **15**, 2405846.
- 26 F. Le, W. Jia, W. Shu, Z. Lu, Y. Lv, T. Wang, X. Wu, X. Yang, F. Ma and D. Jia, *Small*, 2024, **20**, 2404894.
- 27 S. Jeong, Y. Zhang, J. Kang, S. Lee, J. M. Baik and H. Park, *ACS Energy Lett.*, 2025, **10**, 3591–3599.
- 28 P. Ji, R. Yu, P. Wang, X. Pan, H. Jin, D. Zheng, D. Chen, J. Zhu, Z. Pu, J. Wu and S. Mu, *Adv. Sci.*, 2022, **9**, 2103567.
- 29 J. Yao, Y. Zhang, F. Gao, Q. Jin, L. Zhang, L. Xu, M. Zhang, H. Gao and P. Yu, *Energy Environ. Mater.*, 2025, **8**, e70013.
- 30 X.-H. Zhang, M.-T. Zhang, H.-G. Du, H.-H. Huang, X.-F. Zhang, X. Wen, L.-D. Wang, W.-Z. Deng, Y.-M. He, J. Bai, L.-W. Ding and C.-T. He, *Angew. Chem., Int. Ed.*, 2025, **64**, e202507040.
- 31 Y. Xu, Y. Zhao, M. Sun, W. Xie, Y. Wu, G. Cheng, Y. Zhong, S. Han and L. Yu, *Chem. Eng. J.*, 2024, **490**, 151697.
- 32 L. Su, X. Cui, T. He, L. Zeng, H. Tian, Y. Song, K. Qi and B. Y. Xia, *Chem. Sci.*, 2019, **10**, 2019–2024.
- 33 L. Wang, Y. Hao, L. Deng, F. Hu, S. Zhao, L. Li and S. Peng, *Nat. Commun.*, 2022, **13**, 5785.
- 34 H. Wang, X. Shao, Y. Wei, X. Ai, J. Yu, N. Xiao, R. Gan and Y. Qu, *Appl. Catal., B*, 2025, **367**, 125110.
- 35 C. Chen, C. Du, Z. Wang, X. Chen, Y. Wang, N. Ju, Y. Fu, Z. Liu, M. Jia, S. Luo, G. Xu, J. Xu and H.-B. Sun, *Energy Fuels*, 2025, **39**, 12154–12164.
- 36 W. Du, Y. Shi, W. Zhou, Y. Yu and B. Zhang, *Angew. Chem., Int. Ed.*, 2021, **60**, 7051–7055.
- 37 J. A. Bau, H. Haspel, S. Ould-Chikh, A. Aguilar-Tapia, J.-L. Hazemann, H. Idriss and K. Takanabe, *J. Mater. Chem. A*, 2019, **7**, 15031–15035.
- 38 J. A. Bau, S. M. Kozlov, L. M. Azofra, S. Ould-Chikh, A.-H. Emwas, H. Idriss, L. Cavallo and K. Takanabe, *ACS Catal.*, 2020, **10**, 12858–12866.
- 39 J. Nie, J. Shi, L. Li, M.-Y. Xie, Z.-Y. Ouyang, M.-H. Xian, G.-F. Huang, H. Wan, W. Hu and W.-Q. Huang, *Adv. Energy Mater.*, 2025, **15**, 2404246.
- 40 J. Wang, H.-Y. Tan, T.-R. Kuo, S.-C. Lin, C.-S. Hsu, Y. Zhu, Y.-C. Chu, T. L. Chen, J.-F. Lee and H. M. Chen, *Small*, 2021, **17**, 2005713.
- 41 Y. Zhu, K. Fan, C.-S. Hsu, G. Chen, C. Chen, T. Liu, Z. Lin, S. She, L. Li, H. Zhou, Y. Zhu, H. M. Chen and H. Huang, *Adv. Mater.*, 2023, **35**, 2301133.
- 42 X. Ding, D. Liu, P. Zhao, X. Chen, H. Wang, F. E. Oropeza, G. Gorni, M. Barawi, M. García-Tecedor, V. A. de la Peña O'Shea, J. P. Hofmann, J. Li, J. Kim, S. Cho, R. Wu and K. H. L. Zhang, *Nat. Commun.*, 2024, **15**, 5336.
- 43 X. Ding, D. Liu, A. wang, P. Zhang, F. E. Oropeza, P. Zhao, G. Gorni, M. Barawi, V. de la Peña O'Shea, R. Wu and K. H. L. Zhang, *Adv. Funct. Mater.*, 2025, e21566.
- 44 M. Ledendecker, J. S. Mondschein, O. Kasian, S. Geiger, D. Göhl, M. Schalenbach, A. Zeradhanin, S. Cherevko, R. E. Schaak and K. Mayrhofer, *Angew. Chem., Int. Ed.*, 2017, **56**, 9767–9771.
- 45 Y. Zhu, H.-C. Chen, C.-S. Hsu, T.-S. Lin, C.-J. Chang, S.-C. Chang, L.-D. Tsai and H. M. Chen, *ACS Energy Lett.*, 2019, **4**, 987–994.
- 46 K. Fan, H. Zou, N. V. R. A. Dharanipragada, L. Fan, A. K. Inge, L. Duan, B. Zhang and L. Sun, *J. Mater. Chem. A*, 2021, **9**, 11359–11369.



- 47 L. Zhou, C. Yang, W. Zhu, R. Li, X. Pang, Y. Zhen, C. Wang, L. Gao, F. Fu, Z. Gao and Y. Liang, *Adv. Energy Mater.*, 2022, **12**, 2202367.
- 48 A. Zhu, L. Qiao, K. Liu, G. Gan, C. Luan, D. Lin, Y. Zhou, S. Bu, T. Zhang, K. Liu, T. Song, H. Liu, H. Li, G. Hong and W. Zhang, *Nat. Commun.*, 2025, **16**, 1880.
- 49 P. Fang, M. Zhu, J. Liu, Z. Zhu, J. Hu and X. Xu, *Adv. Energy Mater.*, 2023, **13**, 2301222.
- 50 C. Chen, H. Jin, P. Wang, X. Sun, M. Jaroniec, Y. Zheng and S.-Z. Qiao, *Chem. Soc. Rev.*, 2024, **53**, 2022–2055.
- 51 X. Wang, Q. Ruan and Z. Sun, *Energy Fuels*, 2023, **37**, 17667–17680.
- 52 X. Zheng, X. Shi, H. Ning, R. Yang, B. Lu, Q. Luo, S. Mao, L. Xi and Y. Wang, *Nat. Commun.*, 2023, **14**, 4209.
- 53 H. Tan, B. Tang, Y. Lu, Q. Ji, L. Lv, H. Duan, N. Li, Y. Wang, S. Feng, Z. Li, C. Wang, F. Hu, Z. Sun and W. Yan, *Nat. Commun.*, 2022, **13**, 2024.
- 54 D. Bao, L. Huang, Y. Gao, K. Davey, Y. Zheng and S.-Z. Qiao, *J. Am. Chem. Soc.*, 2024, **146**, 34711–34719.
- 55 A. Angulo, P. van der Linde, H. Gardeniers, M. Modestino and D. Fernández Rivas, *Joule*, 2020, **4**, 555–579.
- 56 J. Feng, X. Wang and H. Pan, *Adv. Mater.*, 2024, **36**, 2411688.
- 57 J. M. Gisbert-González, C. G. Rodellar, J. Druce, E. Ortega, B. R. Cuenya and S. Z. Oener, *J. Am. Chem. Soc.*, 2025, **147**, 5472–5485.
- 58 C. Feng, J. Shao, H. Wu, A. Hassan, H. Yang, J. Yu, Q. Hu and C. He, *Chin. J. Catal.*, 2025, **72**, 230–242.
- 59 N. Elgrishi, K. J. Rountree, B. D. McCarthy, E. S. Rountree, T. T. Eisenhart and J. L. Dempsey, *J. Chem. Educ.*, 2018, **95**, 197–206.
- 60 C. Ariño, C. E. Banks, A. Bobrowski, R. D. Crapnell, A. Economou, A. Królicka, C. Pérez-Ràfols, D. Soulis and J. Wang, *Nat. Rev. Methods Primers*, 2022, **2**, 62.
- 61 D. Hochfilzer, A. Tiwari, E. L. Clark, A. S. Bjørnlund, T. Maagaard, S. Horch, B. Seger, I. Chorkendorff and J. Kibsgaard, *Langmuir*, 2022, **38**, 1514–1521.
- 62 N. Mayet, K. Servat, K. B. Kokoh and T. W. Napporn, *Surfaces*, 2019, **2**, 257–276.
- 63 M. Rocca, T. Rahman and L. Vattuone, *Springer handbook of surface science*, Springer Nature, 2021.
- 64 J. Tymoczko, W. Schuhmann and A. S. Bandarenka, *Chem-ElectroChem*, 2014, **1**, 213–219.
- 65 Z. Xiao, Y.-C. Huang, C.-L. Dong, C. Xie, Z. Liu, S. Du, W. Chen, D. Yan, L. Tao, Z. Shu, G. Zhang, H. Duan, Y. Wang, Y. Zou, R. Chen and S. Wang, *J. Am. Chem. Soc.*, 2020, **142**, 12087–12095.
- 66 H.-Y. Wang, S.-F. Hung, H.-Y. Chen, T.-S. Chan, H. M. Chen and B. Liu, *J. Am. Chem. Soc.*, 2016, **138**, 36–39.
- 67 X. Liu, J. Meng, J. Zhu, M. Huang, B. Wen, R. Guo and L. Mai, *Adv. Mater.*, 2021, **33**, 2007344.
- 68 H. S. Magar, R. Y. A. Hassan and A. Mulchandani, *Sensors*, 2021, **21**, 6578.
- 69 Y. Liu, J. Wu, K. P. Hackenberg, J. Zhang, Y. M. Wang, Y. Yang, K. Keyshar, J. Gu, T. Ogitsu, R. Vajtai, J. Lou, P. M. Ajayan, B. C. Wood and B. I. Yakobson, *Nat. Energy*, 2017, **2**, 17127.
- 70 K. Dastafkan, S. Wang, S. Song, Q. Meyer, Q. Zhang, Y. Shen and C. Zhao, *EES Catal.*, 2023, **1**, 998–1008.
- 71 J. Jiang, G. Xu, B. Gong, J. Zhu, W. Wang, T. Zhao, Y. Feng, Q. Wu, S. Liu and L. Zhang, *Adv. Funct. Mater.*, 2025, **35**, 2412685.
- 72 H. Wang, Y. Jiao, G. Zhang, W. Ma, W. Fan, X. Liu, Y. Zhao, H. Xie, W. Ma and X. Zong, *Adv. Funct. Mater.*, 2025, **35**, 2418617.
- 73 Z. Zhao, Y. Chen, Y. Liu, S. Qin, Z. Li, Z. Zhang and X. Meng, *Adv. Funct. Mater.*, 2025, e28280.
- 74 X. Chen, M. Bi, Q. Yan, D. Fan, B. Huang, B. Sun, C. Qin, C. Chen, D. Sun, Q. He and M. Zhao, *Adv. Mater.*, 2025, **37**, e08893.
- 75 J. Kwon, S. Choi, C. Park, H. Han and T. Song, *Mater. Chem. Front.*, 2024, **8**, 41–81.
- 76 L. Zhang, Z. Shi, Y. Lin, F. Chong and Y. Qi, *Front. Chem.*, 2022, **10**, 866415.
- 77 X. Gao, P. Wang, X. Sun, M. Jaroniec, Y. Zheng and S. Z. Qiao, *Angew. Chem.*, 2025, **137**, e202417987.
- 78 R. Lin, Y. Lu, J. Xu, J. Huo and X. Cai, *Appl. Energy*, 2022, **326**, 120011.
- 79 A. Bashkatov, S. Park, Ç. Demirkır, J. A. Wood, M. T. M. Koper, D. Lohse and D. Krug, *J. Am. Chem. Soc.*, 2024, **146**, 10177–10186.
- 80 Q.-N. Wang, Y. Qiao, W. Qin, H. Zheng, Z. Wang, B. Chang, X. Qu, W. Zhang, T. Liu and C. Li, *Ind. Eng. Chem. Res.*, 2025, **64**, 5087–5098.
- 81 B. T. Sangtam and H. Park, *Micromachines*, 2023, **14**, 2234.
- 82 Y. Lin, D. Huang, Q. Wen, R. Yang, B. Chen, Y. Shen, Y. Liu, J. Fang, H. Li and T. Zhai, *Proc. Natl. Acad. Sci. U. S. A.*, 2024, **121**, e2407350121.
- 83 L. Xia, B. F. Gomes, W. Jiang, D. Escalera-López, Y. Wang, Y. Hu, A. Y. Faid, K. Wang, T. Chen, K. Zhao, X. Zhang, Y. Zhou, R. Ram, B. Polesso, A. Guha, J. Su, C. M. S. Lobo, M. Haumann, R. Spatschek, S. Sunde, L. Gan, M. Huang, X. Zhou, C. Roth, W. Lehnert, S. Cherevko, L. Gan, F. P. García de Arquer and M. Shviro, *Nat. Mater.*, 2025, **24**, 753–761.
- 84 X. Liu, J. Meng, K. Ni, R. Guo, F. Xia, J. Xie, X. Li, B. Wen, P. Wu, M. Li, J. Wu, X. Wu, L. Mai and D. Zhao, *Cell Rep. Phys. Sci.*, 2020, **1**, 100241.
- 85 E. Kuhnert, V. Hacker and M. Bodner, *Int. J. Energy Res.*, 2023, **2023**, 3183108.
- 86 P. Aßmann, A. S. Gago, P. Gazdzicki, K. A. Friedrich and M. Wark, *Curr. Opin. Electrochem.*, 2020, **21**, 225–233.
- 87 H.-C. Wu, Y.-W. Huang, Y.-C. Lin, C.-H. Yang and T.-C. Liu, *ACS Appl. Mater. Interfaces*, 2025, **17**, 56991–57001.
- 88 A. Samreen, M. Azim and F. Chen, *AI Mater.*, 2025, **1**, 1–2.
- 89 H. Sheng, J. Sun, O. Rodríguez, B. B. Hoar, W. Zhang, D. Xiang, T. Tang, A. Hazra, D. S. Min, A. G. Doyle, M. S. Sigman, C. Costentin, Q. Gu, J. Rodríguez-López and C. Liu, *Nat. Commun.*, 2024, **15**, 2781.
- 90 C. S. Movassaghi, K. A. Perrotta, M. E. Curry, A. N. Nashner, K. K. Nguyen, M. E. Wesely, M. Alcañiz Fillol, C. Liu, A. S. Meyer and A. M. Andrews, *Digital Discovery*, 2025, **4**, 1812–1832.

